

# Li cation–aromatic organic radical complex in a zeolite studied by electron spin echo envelope modulation spectroscopy

D.C. Doetschman <sup>a,\*</sup>, D.C. Gilbert <sup>a</sup>, D.W. Dwyer <sup>b,1</sup>

<sup>a</sup> Department of Chemistry, Binghamton University, State University of New York, Binghamton, NY 13902-6016, USA

<sup>b</sup> College at Brockport, State University of New York, Brockport, NY 14420, USA

Received 18 February 2000

## Abstract

The <sup>7</sup>Li nuclear resonance correlation spectra of a proposed Li–phenalenyl free radical complex in the interior of the supercages in Li-exchanged Y-type faujasite zeolite at 15 K are presented. The spin Hamiltonian parameters,  $A_{xx}/h = 5.23 \pm 0.02$ ,  $A_{yy}/h = 6 \pm 3$ ,  $A_{zz}/h = 167 \pm 9$  (signs from model),  $|e^2Qq|/h = 1.24 \pm 0.04$  in units of MHz and  $|\eta| = 0.0 \pm 0.2$ , are shown to be consistent with an  $sp^n$  hybrid orbital on the Li ion, strongly associated with an aluminosilicate bridging O, to which the easily polarizable non-bonding, unpaired,  $a_1'$  electron of phenalenyl is partially transferred. The isotropic hyperfine interaction,  $a/h = 59 \pm 2$  MHz, implies that  $16.3 \pm 0.6\%$  of the spin is transferred to the Li 2s orbital. The anisotropic hyperfine interaction, together with the quadrupole interaction, implies that there is a substantial additional spin transferred to the 2p orbital of Li in the O–Li bond direction. © 2000 Elsevier Science B.V. All rights reserved.

## 1. Introduction

Zeolite substances are well known for their ability to sequester organic molecules for a number of applications, including chromatography, adsorption and catalysis. A great deal has been learned about the strengths of the molecule–cage interactions, thereby leading to microscopic models of the interactions [1]. A number of spectroscopic investigations have given a much more specific picture of the molecule–cage interaction

[2–4]. Kasai and Bishop's pioneering work opened up the study of spin–probe interactions with the surfaces of porous solids with electron paramagnetic resonance (EPR) [5]. In recent years, pulsed EPR has been shown to be an important tool for studying molecular dynamics [6], including the dynamics of absorbed paramagnetic molecules [7–9]. Several groups have employed pulsed EPR studies of nitroxide spin probes extensively in order to understand the interactions of solvent molecules, probe molecules and the surfaces in porous solids [10,11].

We have recently turned our attention to the physical and chemical dynamics of organic molecules adsorbed into X- and Y-type faujasite zeolites [12–15]. Studies of phenalenyl-alkali metal cation solutions with nuclear magnetic resonance (NMR) and EPR have shown the existence of  $Li^+$

\* Corresponding author. Tel.: +1-607-777-2298; fax: +1-607-777-4478.

E-mail address: fac238@bingvmb.cc.binghamton.edu (D.C. Doetschman).

<sup>1</sup> Present address: SAIC, POST, Suite 803, 1225 Jefferson Davis Hwy., Arlington, VA 22202, USA.

and  $\text{Na}^+$  complexes with the neutral  $\pi$ -aromatic radical and have measured appreciable cation-phenalenyl association constants.<sup>2</sup> Although these solution studies support the hypothesis that phenalenyl-cation complexes exist, there is only indirect kinetic evidence that such a complex exists in the faujasite zeolite cage [12]. Direct spectroscopic evidence for the existence of this type of complex in the zeolite cage is desirable. Additionally, we have found the EPR spectrum of a tightly bound  $\text{O}_2$  molecule that cannot be removed at elevated temperatures under vacuum [14,16].

In this paper, we present evidence for the Li complex obtained from EPR studies of phenalenyl doped faujasite zeolite cages with the hyperfine sublevel correlation (HYSCORE) technique. HYSCORE is a multiple pulse EPR electron spin echo envelope modulation (ESEEM) coherence technique that has an increasing list of applications especially to nuclei with  $I = 1/2$ . This is largely due to the existence of a straightforward analytical treatment [17] of the two-dimensional (2D) correlation features that appear in the 2D Fourier transform of the HYSCORE experiment with nuclei of spin  $I = 1/2$ . Another advantage of the HYSCORE experiment is its ability to reveal correlation lines spanning substantial frequency ranges in the 2D transform, whose accumulation would be washed out in the one-dimensional analog. ESEEM techniques, of which HYSCORE is a particular type, have achieved widespread use in the study of paramagnetic cations in zeolitic substances, often in the presence of organic dopants [18]. Towards this end, we present our analysis of the HYSCORE correlation features for  $^7\text{Li}$  in phenalenyl-doped LiY. The  $^7\text{Li}$  results will be discussed in terms of the degree to which the covalency of the phenalenyl-cation complexes results in the transfer of unpaired electron spin density to the cation. The anisotropy of the phenalenyl-cation nucleus hyperfine interaction will also be discussed in terms of transferred electron

spin among the cation 2s and 2p atomic orbitals from the phenalenyl  $\pi$  system.

## 2. Experimental details

The preparation of the phenalenyl-doped, Li cation-exchanged Y-type zeolite has been described elsewhere [12,14]. Samples of the alkali metal cation-exchanged [14] Y-faujasite zeolite were loaded with phenalene, the phenalenyl precursor, via hexane solvent [12]. Some of the samples from the previous study [14] were used in this work. Additional and replacement samples were similarly prepared from zeolites whose cation exchange and characterization were described in a study of nitroxide spin probe dynamics [15]. Undoped samples were also examined.

Four-pulse HYSCORE experiments were performed on a Bruker ESP 580 system with a split-ring Bruker ER4AA9 (optical) resonator operating in overcoupled, low Q mode. The system was equipped with an Oxford CF935 cryostat, operating with an Oxford Instruments ITC 502 controller referenced to boiling  $\text{N}_2(\text{l})$ . In all experiments, the laboratory magnetic field was tuned to the center of the phenalenyl hyperfine pattern. The four-pulse HYSCORE experiments were done at 8 or 15 K with a non-ideal 16–16–24–16 ns pulse sequence with the equal microwave pulse amplitudes adjusted independently for a maximum Hahn echo with a 16–24 ns pulse sequence. We have found the 16–16–24–16 ns pulse sequence advantageous in observing intramanifold correlations in certain cases [19]. The first pulse interval was  $\tau = 130$ –138 ns for phenalenyl proton resonance suppression and the second and third pulse intervals  $T_1$  and  $T_2$  were incremented from 40 ns at 24 ns intervals to achieve a  $128 \times 128$  array of echo intensity measurements. A number of three- and four-pulse experiments were performed with  $\tau = 98$ –104 ns to enhance the proton resonances in order to show that the observed resonances assigned to cations were not in fact proton resonances. Pairs of HYSCORE experiments with proton enhancement and suppression were performed on NaX and NaY samples to ascertain whether residual Na left in Li-exchanged zeolites

<sup>2</sup> D.W. Dwyer, M.F. Ciruolo, D.C. Gilbert, D.C. Doetschman, unpublished work on a magnetic resonance study of complex formation between the phenalenyl radical and alkali metal ions in dilute alcohol solutions.

could be responsible for the resonances assigned to Li. Examinations of LiX, LiY, NaX, and NaY zeolites with selective nuclear suppression in similarly performed three-pulse ESEEM experiments were performed at 40 K.

The echo decay modulations were pre-processed for later spectrum analysis as follows and Fourier transformed. The four-pulse HYSORE echo decays were processed by subtraction of best-fit quadratic or cubic equations, zero filled in both the  $T_1$  and  $T_2$  dimensions to  $256 \times 256$  arrays, apodized with a Hamming window function in both dimensions to smooth the transition into the zero-filled region and fast Fourier transformed in two dimensions. These manipulations were performed with Bruker XEPR pulsed EPR software, and the correlation features were measured from contour plots with a cursor and recorded. Thus, the basic data for further analysis was in the form of  $(\nu_1, \nu_2)$  points, and their respective relative absolute value spectral intensities, where  $\nu_1$  is the Fourier transform of the  $T_1$  dimension and  $\nu_2$  is the transform coordinate of the  $T_2$  dimension. The  $\nu_1$  and  $\nu_2$  correspond to correlations between nuclear resonance intervals in the  $\alpha$  (or  $\beta$ ) electron spin manifold with those in the  $\beta$  (or  $\alpha$ ) manifold. The assignment of  $\nu_1$  to  $\pm\nu_\alpha$  or  $\pm\nu_\beta$  for a particular feature in the spectrum is ambiguous without further analysis and likewise for assignment of  $\nu_2$ . The three-pulse ESEEM experiments were pre-processed in a similar manner with linear phase correction.

### 3. Experimental results

The 15-K HYSORE spectrum of phenalenyl-doped LiY zeolite is shown in Fig. 1. Of particular interest are the off diagonal features between  $\approx(-8.5, 3.0)$  and  $(-12.5, 8.3)$  MHz, and their reflection features across the  $(-, +)$  quadrant diagonal,  $\approx(-4.0, 8.0)$  to  $(-8.0, +12.5)$  MHz. Corresponding features were not found in the LiX, NaX and NaY hosts. The features in LiY decrease rapidly with increasing temperatures and disappear by 25 K. The  $^6\text{Li}$  correlations in LiY are not strong enough to be observed at natural abundance.

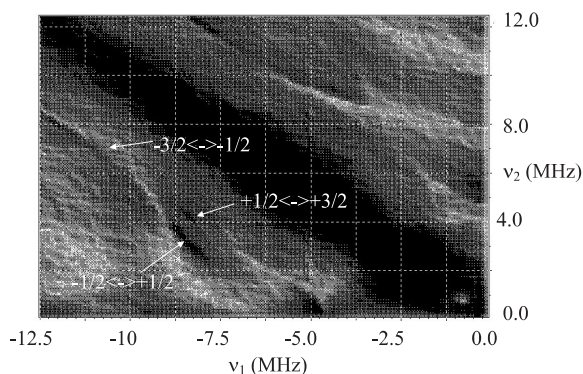


Fig. 1. HYSORE spectrum of Li-phenalenyl complex in Li-exchanged Y zeolite. The horizontal frequency coordinate  $\nu_1$  corresponds to the  $T_1$  interval of the pulse sequence and the vertical frequency coordinate  $\nu_2$  corresponds to the  $T_2$  interval of the pulse sequence. The intensity scale of the frequency correlation is a logarithmic gray scale with the white indicating the lowest, and the black indicating the highest relative intensities. The assignments to particular electron spin manifolds are shown in Fig. 2.

In the three-pulse ESEEM experiments at 40 K, a sharp peak at the  $^7\text{Li}$  nuclear resonance frequency is observed in Li-exchanged zeolite, together with sharp, overlapping peaks near the  $^{27}\text{Al}$  and  $^{23}\text{Na}$  frequencies. Enhancement of one of the sharp peaks near the  $^{23}\text{Na}$  frequency is observed in the Na-exchanged zeolite. Broad phenalenyl  $^1\text{H}$  features and a  $^1\text{H}$  matrix resonance are present in all spectra. Again, the  $^6\text{Li}$  resonance is evidently not strong enough to be observed at natural abundance.

### 4. Analysis

The LiY HYSORE features were assigned to  $^7\text{Li}$  resonances. The analysis points to correlations between corresponding single quantum nuclear resonances in the two-electron spin manifolds (of Li-phenalenyl complex). The observed correlations were found to originate from field orientations near the perpendicular plane of an approximately axial Li nuclear hyperfine coupling A. The correlations were fit by the Hamiltonian,

$$H = g|\beta e|HS - g_n\beta_n HI + SAI + IQI. \quad (1)$$

In actual practice, the Hamiltonian was solved in the high-field approximation, reducing the problem to two  $4 \times 4$  nuclear spin blocks for  $I = 3/2$   $^7\text{Li}$  nucleus, one for the upper electron spin manifold and one for the lower manifold. Nuclear transition frequencies were calculated from the eigenvalues and the intensities of the correlation features were calculated from the nuclear spin eigenvectors [20]. Calculations were programmed in Mathcad Professional Version 7.03.

Preliminarily, we assumed co-axial axial symmetry for  $A$  and  $Q$ . Parameters of  $a/h = \pm 51.3$  ( $\pm 0.3$ ) MHz,  $T/h = \pm 46$  ( $\pm 2$ ) MHz and  $|e^2qQ/12h| = 0.5$  ( $\pm 0.1$ ) MHz were found by adjusting for an approximate simulation of calculated and observed HYSCORE frequency correlation ridges. (These parameters are related to the spin Hamiltonian parameters by  $A_{xx} = A_{yy} = a - T$  and  $A_{zz} = a + 2T$ .) The  $A$  (or  $a$  and  $T$ ) values dictate that one is far from the cancellation condition at which ESEEM intensities are appreciable, except for fields near the  $xy$  plane normal to the assumed cylindrical axis  $z$  of the hyperfine coupling. The relatively large hyperfine coupling constants in comparison with the  $^7\text{Li}$  nuclear Zeeman frequency are consistent with the appearance of predominant correlation features in the  $(-, +)$  quadrant. Data points measured from the ridges of the HYSCORE correlation features with the Bruker software cursor are shown in Fig. 2 in comparison with the final best fit correlations predicted from theory. One does not observe the usual arcing HYSCORE features sometimes crossing the diagonal of the quadrant, ordinarily associated with  $^7\text{Li}$  HYSCORE in systems with small hyperfine coupling constants [21]. The three, approximately parallel HYSCORE ridges observed are assigned to correlations between each ( $m_I \leftrightarrow m_I + 1$ ) nuclear resonance frequency in the upper electron spin manifold with the same ( $m_I \leftrightarrow m_I + 1$ ) nuclear resonance in the lower electron spin manifold (Fig. 2).

The experimental ridge points represent the maximum intensities found along some arbitrary coordinate, such as  $\nu_\alpha$  or  $\nu_\beta$ . We explain here the method by which we calculate the coordinates of a theoretical ridge curve with which refinement of

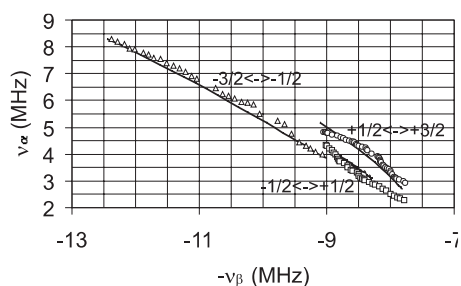


Fig. 2. The correlation ridge points measured from the contour presentation of the HYSCORE spectrum of the Li–phenalenyl complex in Li-exchanged Y zeolite shown in Fig. 1. The particular assignments of the correlation features to the observed single quantum–single quantum nuclear transitions are shown, together with an assignment of the observed frequencies to particular electron spin manifolds in the axis labels. Also shown are the correlation ridge lines predicted from the best fit of the Hamiltonian to the experimental ridge points.

the spin Hamiltonian parameters was performed. For a given set of parameters and a particular field direction and strength, Hamiltonian (1) was solved in the high-field approximation for the nuclear spin eigenvalues and eigenfunctions for  $m_s = \pm 1/2$  states. The eigenvalues were energy ordered and the desired, assigned nuclear transition frequencies were determined. The nuclear spin eigenvectors were used to calculate the relative intensities of the assigned correlations at the particular field and direction [20]. As these intensities are effectively on a per unit solid angle basis, they can be viewed as values of  $1/\sin\theta \partial^2 I / \partial\theta \partial\phi$  in polar coordinates. On the other hand, the observed intensities are effectively on a per unit squared frequency basis, the units of  $\nu_\alpha \times \nu_\beta$ . In order to calculate relative intensities in the two-dimensional frequency plane, appropriate angular increments in polar coordinates were made and the corresponding increments in  $\nu_\alpha$  and  $\nu_\beta$  were determined by successive solutions of the Hamiltonian. Thus, a numerical evaluation of  $\sin\theta \partial\theta \partial\phi / \partial\nu_\alpha \partial\nu_\beta$  was determined with which the calculated value of  $1/\sin\theta \partial^2 I / \partial\theta \partial\phi$  could be converted to the desired value of  $\partial^2 I / \partial\nu_\alpha \partial\nu_\beta$ .

In this way, a series of relative intensities was calculated for every value of the field projection angle,  $0 < \theta < \pi$ , in suitable, equal increments and for every value of the field projection angle,

$0 < \phi < \pi$ , in suitable increments proportional to  $\sin \theta$ . The intensity values at a given  $\theta$  for the various  $\phi$  values were searched for the maximum intensity. From these maxima, the theoretical ridge intensities,  $I(\theta)$ , and the ridge angular coordinates thus defined,  $\phi(\theta)$ , the theoretical ridge correlation frequencies  $\nu_\alpha(\theta)$ ,  $\nu_\beta(\theta)$  were generated for comparison with experiment, all expressed as functions of the single variable  $\theta$ . The spin Hamiltonian parameters were varied systematically, beginning with the approximate values above, until a minimum was obtained in the sums of the squares of the distances (in  $\text{Hz}^2$ ) from the data points to the theoretical line of  $\nu_\beta$  versus  $-\nu_\alpha$ . The results of the least squares fit, assuming that the principal axes of the quadrupole and hyperfine interactions are parallel, are given in Table 1. The table gives the final values and uncertainties in the spin Hamiltonian parameters. Although the initial assumption of axial symmetries was relaxed, it is seen that axial symmetry does indeed prevail within experimental error. With this result, it does not appear likely that there is substantial deviation between the quadrupole and hyperfine axis systems. An independent check on a possible value of  $A_{yy} \gg A_{xx}$  showed that the result in Table 1 with  $A_{xx} \sim A_{yy}$  is the true minimum of the fit. The surprising, weaker dependence of the results on  $A_{yy}$  than  $A_{xx}$ , as indicated by their respective standard deviations,  $\sigma$ , is a consequence of the handedness of the intensity behavior.

Table 1

Best values of the spin Hamiltonian (1) parameters for the  $^7\text{Li}$ -phenalenyl complex in Li-exchanged Y zeolite obtained by a least squares fit of the calculated frequency correlation ridges to the experimental values for the correlations between each  $(m_l \leftrightarrow m_l + 1)$  nuclear resonance frequency in the  $\alpha$  electron spin manifold with the negative of the  $(m_l \leftrightarrow m_l + 1)$  nuclear resonance frequency in the  $\beta$  electron spin manifold (Fig. 2)<sup>a</sup>

Parameter	Value	$\sigma$
$A_{xx}/h$	$\pm 5.23$ MHz	0.02 MHz
$A_{yy}/h$	$\pm 6$ MHz	3 MHz
$A_{zz}/h$	$\pm 167$ MHz	9 MHz
$ e^2Qq /h$	1.24 MHz	0.04
$ \eta $	0.0	0.2

<sup>a</sup>The asymmetry parameter,  $\eta = (Q_{xx} - Q_{yy})/Q_{zz}$ . The standard deviations,  $\sigma$ , of each value are also given.

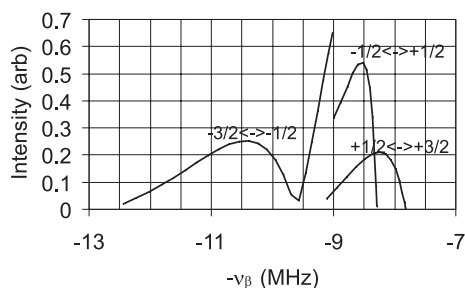


Fig. 3. The absolute value intensities along the corresponding correlation ridge lines of Fig. 2 predicted from the best fit of the Hamiltonian to the experimental ridge points against the same  $\nu_\beta$  scale.

Plots of the best fit theoretical intensities of the three-correlation ridges are shown in Fig. 3 as functions of  $-\nu_\alpha$  for comparison with the correlation ridges in Fig. 2. There actually exist nuclear resonances  $\nu_\alpha$  and  $\nu_\beta$  with frequencies whose magnitudes are much higher than those shown in Fig. 2 that result from field directions approaching the  $z$  axis, where  $A_{zz} = \pm 167$  MHz. However, the intensities of the resonances decrease rapidly outside the small region of the experimentally observed correlation ridges deriving from fields near the  $xy$  plane, as can be seen in Fig. 3.

A comment is perhaps in order concerning the efficiency and the advantages of the present approach to the analysis of ESEEM data. Firstly, the magnitude of the computational effort made here is no less than would be required to calculate the whole 2D-ESEEM spectrum;  $I(\theta, \phi)$ ,  $\nu_\alpha(\theta, \phi)$ , and  $\nu_\beta(\theta, \phi)$  have, in fact, all been calculated. In general, however, there is a frequent occurrence of overlapping correlations between different transitions of a given nucleus in ESEEM spectra. Moreover, the correlations of different nuclei or the same nuclei in different environments may overlap. Finally, the data preparation and Fourier transformation processes may not yield perfectly flat baseplanes for the experimental  $I(\nu_\alpha, \nu_\beta)$  plot. For these reasons, we have found it advantageous to focus on the comparison of experimental and theoretical ridge coordinates of isolated correlations or isolated sets of correlations, thus reducing the dimensionality of the data analysis. The vicinities of the ridges are, after all, where most of the information in the spectrum lies.

## 5. Discussion

The results suggest that a Li–phenalenyl complex is formed in which substantial spin density is transferred from the non-bonding  $\pi$  orbital of phenalenyl into an  $sp$  hybrid orbital of the Li. One would expect the charge compensating Li ion to be situated on an oxygen atom that bridges to an aluminum ion of the aluminosilicate structure of the zeolite (Fig. 4). The structure of a site of this type has been determined by HYSORE for a  $\gamma$ -radiation defect center in a lithium silicate [21]. A structure that is consistent with the present results is shown in Fig. 4. The isotropic hyperfine coupling constant determined from Table 1 is  $a/h = \pm 59 \pm 2$  MHz. This value with the positive sign choice, together with the theoretical value for unit spin in a Li 2s orbital [22], indicates that about  $16.3 \pm 0.6\%$  of the electron spin resides in the Li 2s orbital. Then, the anisotropic part of the hyperfine interaction is nearly axial in symmetry with  $T_{\parallel}/h = 108 \pm 4$  MHz and  $T_{\perp}/\eta = -54 \pm 2$  MHz. The magnitude and signs of  $T_{\parallel}$  and  $T_{\perp}$  are consistent with spin density in a 2p orbital of the Li. The quadrupole parameters show that the direction of the major electric field gradient is parallel to this p orbital direction.

One would expect the major quadrupole axis of Li to point toward the oxygen atom with which it is tightly associated. Thus, its magnitude might be expected to be large, as observed, if the Li–O interaction is substantially covalent. The quadrupole interaction,  $|e^2qQ|/h$ , reported by Astrakas et al. for the  $^7\text{Li}$ , in an evidently more ionic center in the lithium silicate glass, was  $< 0.2$  MHz [21]. The

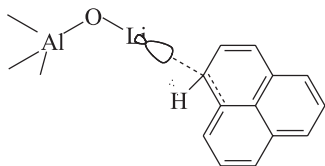


Fig. 4. Schematic diagram of the proposed structure of the Li–phenalenyl complex at a bridging oxygen of the aluminosilicate structure on the interior of a Li-exchanged zeolite supercage. The  $sp^n$  hybrid of Li observed to contain electron spin transferred from the phenalenyl free radical is shown.

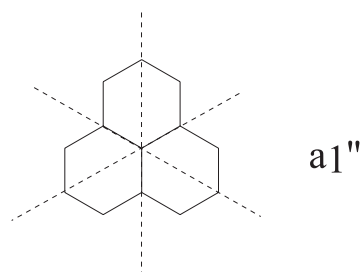
coaxial  $A$  and quadrupole interactions are satisfied in a picture in which the Li  $sp$  hybridization opposes the Li–O bond, which in turn might be expected to have complementarily more Li 2s character and less 2p character.

The determination of the amount of Li 2p character in the hybrid from the experimentally determined anisotropic hyperfine interaction is problematic. We are aware of no theoretical calculations and few experimental determinations that yield a value for the anisotropic hyperfine interaction per unit spin in a Li 2p orbital. An anisotropic hyperfine interaction has been measured by Kasai for an end-on HCN–Li complex [23]. Kasai has also performed a MINDO calculation on the complex that predicts the Li 2p spin density [23]. An  $sp$  hybridization that agrees with both the signs and magnitude of the measured anisotropic coupling gives  $T_{\parallel}/h = -2T_{\perp}/\eta = 234$  MHz per unit spin in a Li 2p orbital. One should take this value with caution, however, as the size of the Li 2p spin density from the MINDO calculation was a small 0.04. On this basis, our observed anisotropic hyperfine interaction would correspond to a Li 2p spin density of nearly 0.5. Thus, it is safe to say that the  $sp$  hybrid has a significant p character [24].<sup>3</sup>

We are fortunate indeed to have observed this spectrum, in which two hyperfine interaction elements,  $A_{xx}$  and  $A_{yy}$ , approach so closely the cation nuclear resonance frequency, thereby giving significant HYSORE intensity in the window of observation. We observed no resonance from the phenalenyl–Na complex in NaX or NaY. We will be indeed lucky if we find the HYSORE of the K, Rb, or Cs complexes in the planned future experiments.

The phenalenyl is actually well poised to donate its unpaired electron to an electron acceptor. A simple symmetry molecular orbital analysis shows that the unpaired electron resides in an  $a_1'$  orbital,

<sup>3</sup> Ref. [24] describes  $\pi$  complexes of Li atoms with acetylene and ethylene which exhibit substantial Li 2p unpaired spin density. The anisotropic coupling constant in the present work is surprisingly large by comparison. This is presumably due to Li 2p orbital collapse in the ionic Li adjacent to the electron withdrawing O atom.



Scheme 1.

as shown in Scheme 1. The unpaired electron actually has little resonance stabilization in this orbital due to the nodes that pass between the alternate carbons. The electron can be moved to a more localized region of the molecule near the Li ion with relatively little energy loss. To the extent that the covalent interaction between the Li sp hybrid and the phenalenyl  $\pi$  system dictates, unpaired electron density may be partially transferred to the Li ion, as observed.

The observed temperature dependence, in which the  $^7\text{Li}$  HYSCORE spectrum of the Li–phenalenyl complex is lost above 15 K and appears as a relatively sharp  $^7\text{Li}$  resonance in the 40 K ESEEM spectrum, agrees qualitatively with our model for the motion and binding of phenalenyl to the interior cations of the zeolite supercage [12]. The phenalenyl is proposed to bind via a weak, singly occupied, bonding orbital between the phenalenyl  $\pi$  system and a cation orbital. It is proposed [12] that phenalenyl begins to reorient about the Li at very low temperatures. This is observed to increase electron spin dephasing [12], which is presumably responsible for the loss of the HYSCORE spectrum. The process evidently also averages out the  $^7\text{Li}$  hyperfine interactions.

### Acknowledgements

We are grateful for the support of the Chemistry Program of the National Science Foundation under grants CHE9512274 and CHE9705563. Summer research fellowships for D.C.G. from the Department of Chemistry, Binghamton

University, and a K. Keith Innes summer research fellowship for D.C.G. are gratefully acknowledged.

### References

- [1] R.M. Barrer, *Zeolites and Clay Minerals as Sorbents and Molecular Sieves*, Academic Press, New York, 1978.
- [2] M.A. Hepp, V. Ramamurthy, D.R. Corbin, C. Dybowski, *J. Phys. Chem.* 96 (1992) 2629.
- [3] V. Ramamurthy, J.V. Caspar, D.R. Corbin, B.D. Schlyer, A.H. Maki, *J. Phys. Chem.* 94 (1990) 3391.
- [4] V. Ramamurthy, D.F. Eaton, J.V. Caspar, *Accounts Chem. Res.* 25 (1992) 299.
- [5] P. Kasai, R.J. Bishop Jr., in: J.A. Rabo (Ed.), *Zeolite Chemistry and Catalysis*, ACS Monograph No. 171, American Chemical Society, Washington, DC, 1976, p. 350.
- [6] G.L. Millhauser, J.H. Freed, *J. Chem. Phys.* 81 (1984) 37.
- [7] L.J. Schwartz, G.L. Millhauser, J.M. Freed, *Chem. Phys. Lett.* 127 (1986) 60.
- [8] G.L. Millhauser, J. Gorcester, J.M. Freed, in: J.A. Weil (Ed.), *Electron Magnetic Resonance of the Solid State*, Canadian Society for Chemical Publication, Ottawa, Ont., 1987, p. 571.
- [9] A.N. Kudryashov, S.A. Dzuba, R.I. Smailova, G.A. Markaryan, Ye.V. Lunina, Yu.D. Tsvetkov, *J. Magn. Reson. A* 105 (1993) 204.
- [10] L. Kevan, M. Narayana, in: G.D. Stucky, F.G. Dwyer (Eds.), *Intrazeolite Chemistry*, ACS Symposium Series 218, American Chemical Society, Washington, DC, 1982, p. 283.
- [11] M. Romanelli, M.F. Ottaviani, G. Martini, L. Kevan, *J. Phys. Chem.* 93 (1989) 317.
- [12] D.C. Doetschman, D.W. Dwyer, J.D. Fox, C.K. Frederick, S. Scull, G.D. Thomas, S.G. Utterback, J. Wei, *Chem. Phys.* 185 (1994) 343.
- [13] D.C. Doetschman, G.D. Thomas, *Chem. Phys. Lett.* 232 (1995) 242.
- [14] R.P. Borkowski, D.C. Doetschman, J.D. Fox, G. Gargosian, *Solid State Ionics* 100 (1997) 95.
- [15] D.C. Doetschman, G.D. Thomas, *Chem. Phys.* 228 (1998) 103.
- [16] H. Kon, *J. Am. Chem. Soc.* 95 (1973) 1045.
- [17] S.A. Dikanov, M.K. Bowman, *J. Magn. Reson. A* 116 (1995) 125.
- [18] G. Martini, M.F. Ottaviani, M. Romanelli, L. Kevan, *Colloids and Surf.* 41 (1989) 149.
- [19] R. Szosenfogel, D. Goldfarb, *Mol. Phys.* 95 (1998) 1295.
- [20] J.J. Shane, P. Hoefler, E.J. Reijerse, E. de Boer, *J. Magn. Reson.* 99 (1992) 596.
- [21] L. Astrakas, Y. Deligiannakis, G. Mitrikas, G. Kordas, *J. Chem. Phys.* 109 (1998) 8612.
- [22] J.R. Morton, K.F. Preston, *J. Magn. Reson.* 30 (1978) 577.
- [23] P.H. Kasai, *J. Am. Chem. Soc.* 120 (1998) 7884.
- [24] L. Manceron, A. Schrimpf, T. Boremann, R. Rosendahl, F. Faller, H.-J. Stoeckmann, *Chem. Phys.* 169 (1993) 219.